

Evaluation of MM5-EMICAT2000-CMAQ performance and sensitivity in complex terrain: High-resolution application to the northeastern Iberian Peninsula

Pedro Jiménez^{a,b,*}, Oriol Jorba^{a,b}, René Parra^b, José M. Baldasano^{a,b}

^aBarcelona Supercomputing Center-Centro Nacional de Supercomputación (BSC-CNS), Jordi Girona 29, 08034 Barcelona, Spain

^bLaboratory of Environmental Modeling, Universitat Politècnica de Catalunya (LMA-UPC), Avda. Diagonal 647 10.23, 08028 Barcelona, Spain

Received 3 March 2005; received in revised form 19 October 2005; accepted 22 December 2005

Abstract

The complex configuration of the northeastern Iberian Peninsula (NEIP) provokes a complex behavior of photochemical pollutants, which demands a high spatial resolution when applying an air quality model. CMAQ has been used for air quality assessment in the NEIP coupled with the MM5 meteorological model and EMICAT2000 emission model, and has been extensively evaluated against available ambient data during a typical summertime photochemical pollution episode. Simulations with different resolutions were evaluated to select the needed grid resolution. Meteorological inputs are sensitive to the degree of topographical smoothing. Fine-resolution simulations present the best scores during the development of the sea breeze. The performance of statistical parameters for ground-level O₃ greatly improves when decreasing the horizontal and vertical grid spacing. Statistical parameters indicate that decreasing the horizontal grid spacing to 2 km greatly improves the critical success index, the false alarm ratio and the probability of detection. Furthermore, sensitivity studies provide the opportunity to check whether O₃ values react consistently to similar changes in emissions. The model sensitivity was evaluated by performing simulations to represent O₃ formation with baseline emission rates for VOCs and NO_x, and reducing anthropogenic VOC and NO_x emissions by 35%. Evaluation of ground-level O₃ shows a good agreement when the model predicts dominant VOC-sensitive chemistry. Statistical parameters of O₃ evaluation worsen when reducing VOCs emissions and improve in the—35% NO_x case, indicating that the O₃-production chemistry may not be sufficiently reactive.

© 2006 Elsevier Ltd. All rights reserved.

Keywords: Ozone; Air quality modeling; Model evaluation; Photochemistry; Air pollution

1. Introduction

The northeastern Iberian Peninsula (NEIP) is located in the Western Mediterranean Basin (WMB) and has complex topography. The topography of the study domain is organized from three structural units forming a fan-shape formation

*Corresponding author. Barcelona Supercomputing Center-Centro Nacional de Supercomputación (BSC-CNS), Jordi Girona 29, 08034 Barcelona, Spain. Tel.: +34 934134050; fax: +34 93340255.

E-mail address: pedro.jimenez@bsc.es (P. Jiménez).

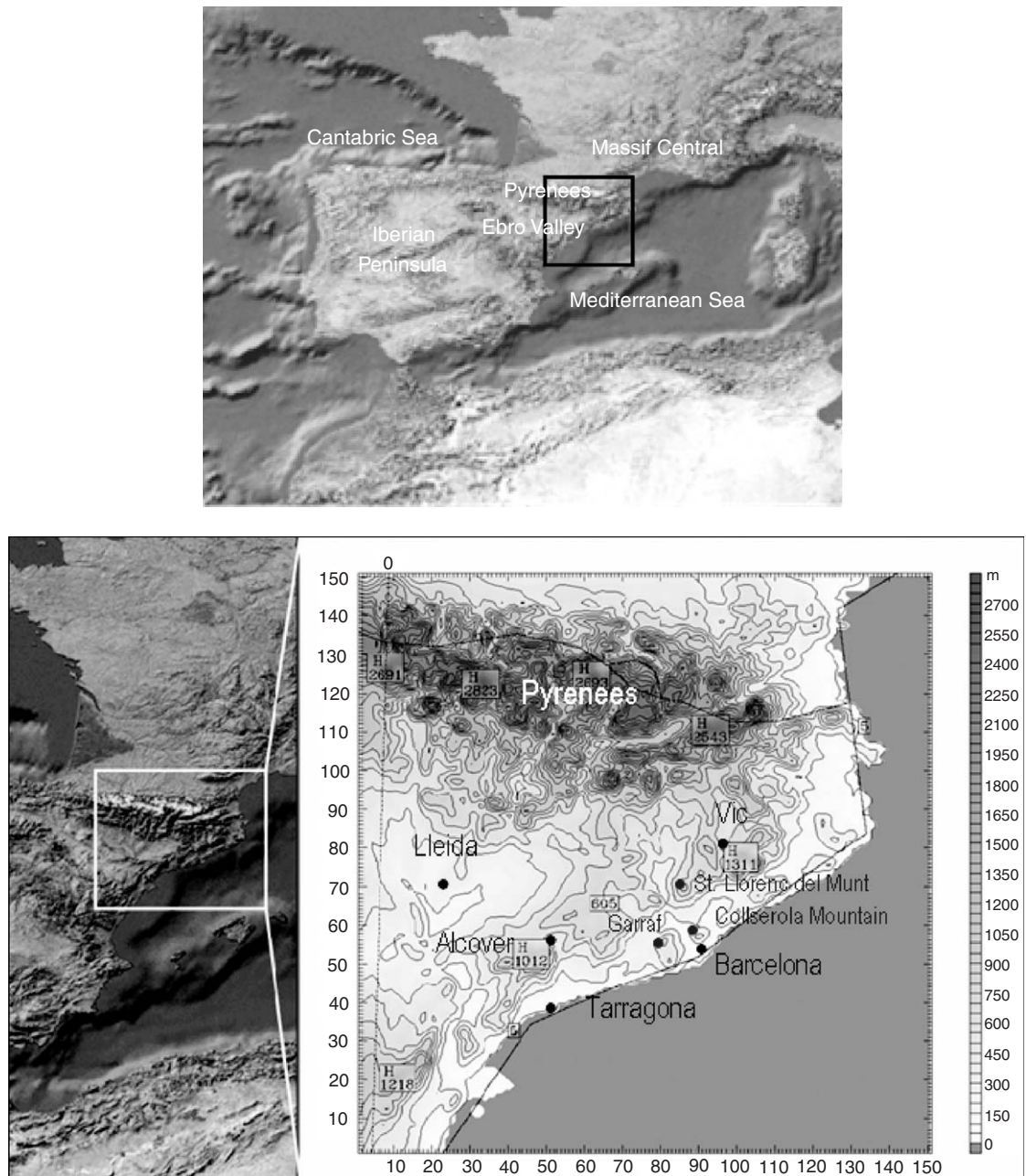


Fig. 1. Location of the northeastern Iberian Peninsula within the Western Mediterranean Basin (top). Relief and main geographical features in the area of study (bottom).

(Fig. 1): the Pyrenees (with altitudes over 3000 m); (2) the Central Valley (or Depression), that stretches all interior zones; and (3) the Mediterranean System, formed by a series of mountain ranges and valleys parallel to the coast. All these topographic features come conditioned by the influence of the Mediterranean Sea and the large valley canalization of Ebro River. The complexity of the

NEIP induces an extremely complicated structure of the flow because of the development of mesoscale phenomena that interact with synoptic flows (superposition of circulations of different scale). The characteristics of the breezes have important effects in the dispersion of emitted pollutants. In addition, the flow can be even more complex because of the heterogeneity of the terrain, the land-use and the

types of vegetation. Therefore, air pollution studies in complex terrain require high-resolution modeling of air quality for resolving complex structures such as flow channeling in valleys or the influence of line and point sources (Kessler et al., 2001; Jiménez et al., 2005a).

Results shown here assess the performance of MM5-EMICAT2000-CMAQ air quality system when applied to the NEIP. This model has been extensively evaluated against available field measurements and air quality stations data for a typical summertime episode of photochemical pollution (Jorba et al., 2004). In order to select the needed resolution for assessing photochemical processes in complex terrain as the NEIP, horizontal resolutions ranging from 8, 4 and 2 km; and 6 and 16 vertical layers were considered, with the height of the first layer at 150 and 36 m above ground level (agl), respectively. Finally, sensitivity studies of ozone response to precursors' controls were performed to define chemically limited regimes in the area.

2. Methods

2.1. MM5-EMICAT2000-CMAQ

The MM5 numerical weather prediction model (Dudhia, 1993) has been used to simulate the mesoscale meteorology. The MM5 options used for the simulations were: Mellor–Yamada scheme as used in the Eta model for the planetary boundary layer (PBL) parameterization; Anthes–Kuo and Kain–Fritsch cumulus scheme; Dudhia simple ice moisture scheme, the cloud-radiation scheme, and the five-layer soil model. Initial and boundary conditions for the simulations were derived from a one-way nested simulation covering a domain of $1392 \times 1104 \text{ km}^2$ centered in the Iberian Peninsula (D1), and data were introduced with analysis data of the European Centre of Medium-range Weather Forecasts global model (ECMWF). Data were available at a 1 degree resolution (about 100 km at the NWMB latitude) at the standard pressure levels for every 6 h.

The high resolution (1 h and 1 km^2) EMICAT2000 emission model (Parra, 2004) has been applied in the NEIP. Biogenic emissions were estimated using a methodology that takes into account local vegetation data (land-use distribution and biomass factors) and meteorological conditions (surface air temperature and solar radiation) together with emission factors for native Mediterranean species and cultures (Parra et al., 2004). On-

road traffic emissions were estimated using the emission factors of the European model EMEP/CORINAIR-COPERTIII (Ntziachristos and Samaras, 2000) as a basis, and differencing the vehicle park composition between weekdays and weekends (Jiménez et al., 2005b). Industrial emissions include real records of some stacks connected to the air quality network of the Environmental Department of the Catalonia Government (Spain), and the estimated emissions from power stations, cement factories, refineries, olefins plants, chemical industries and incinerators.

The chemical transport model used to compute the concentrations of photochemical pollutants for the episode of 13–16 August, 2000, was CMAQ (Byun and Ching, 1999). The mother domain (D1) used EMEP emissions corresponding to year 2000 (www.emep.int) for the photochemical simulations. The chemical mechanism selected was CBM-IV (Gery et al., 1989).

2.2. Statistical evaluation against ambient data

Despite a surface measurement represents a value only at a given horizontal location and height, while the concentration predicted by the model represents a volume-averaged value, performance of the models was statistically evaluated by comparing the first-layer simulations results and the values measured in the meteorological and air quality stations of the domain under study. For evaluation purposes, the results from the meteorological model were compared with surface and aloft wind measurements. Validation data of 52 surface stations located across the domain, and a radiosonde launched in the city of Barcelona (in the center of the domain in the coast) were used. Air quality stations hourly data averaged over the study domain were used in order to report evaluation parameters for CMAQ. Hourly measures of ground-level ozone (O_3), nitrogen oxides (NO_x) and carbon monoxide (CO) were provided by 48 air quality surface stations which belong to the Environmental Department of the Catalonia Government (Spain).

The US Environmental Protection Agency has developed guidelines (US EPA, 1991) drawn from Tesche et al. (1990). Those statistics are: mean normalized bias error (MNBE), mean normalized gross error (MNGE) for concentrations above a prescribed threshold, and unpaired peak prediction accuracy (UPA). Observation/prediction pairs were

excluded from the analysis when the observed concentration was below a cut-off level of 60 ppb (Hogrefe et al., 2001). Other statistical parameters used to evaluate O₃, NO_x and CO in the NEIP are defined in Table 1. These discrete statistics measure the skill of the model when performing diagnostic analyses of pollutant concentrations at specific points (where air quality stations are located). Categorical statistics as derived from Kang et al. (2003; 2004) have also been used to evaluate the different vertical and horizontal grid spacing, including parameters such as the model accuracy (*A*), bias (*B*), probability of detection (POD), false alarm rates (FAR) and critical success index (CSI).

3. Case study: 13–16 August 2000

Modeling was conducted for the photochemical pollution event in the WMB that took place on

13–16 August 2000, when values over the European threshold of 90 ppb (180 μg m⁻³) for ground-level O₃ are attained. The study domain (Fig. 1) covers a squared area of 272 × 272 km² centered in the NEIP (D2). This episode corresponds to a typical summertime low-pressure gradient with high levels of photochemical pollutants over the Iberian Peninsula. These days were characterized by a weak synoptic forcing, so that mesoscale phenomena, induced by the particular geography of the region would be dominant. A high sea level pressure and almost non-existent surface pressure gradients over the domain characterize this day, with slow north-westerlies aloft. This situation is representative of an episode of photochemical pollution in the WMB, since the occurrence of regional re-circulations at low levels represents 45% of the yearly (and 78% of summertime days) transport patterns over the area of study (Jorba et al., 2004). These situations

Table 1
Definition of statistic parameters used for model evaluation^a

Mean bias (MB)	$MB = \frac{1}{N} \sum_1^N (\text{Model} - \text{Obs})$
Mean normalized bias error (MNBE)	$MNBE = \frac{1}{N} \sum_1^N \left(\frac{\text{Model} - \text{Obs}}{\text{Obs}} \right) \times 100\%$
Mean fractionalized bias (MFB)	$MFB = \frac{1}{N} \sum_1^N \left(\frac{\text{Model} - \text{Obs}}{(\text{Model} + \text{Obs} / 2)} \right) \times 100\%$
Mean absolute gross error (MAGE)	$MAGE = \frac{1}{N} \sum_1^N \text{Model} - \text{Obs} $
Mean normalized gross error (MNGE)	$MNGE = \frac{1}{N} \sum_1^N \left(\frac{ \text{Model} - \text{Obs} }{\text{Obs}} \right) \times 100\%$
Normalized mean error (NME)	$NME = \frac{\sum_1^N \text{Model} - \text{Obs} }{\sum_1^N \text{Obs}} \times 100\%$
Normalized meanbias (NMB)	$NMB = \frac{\sum_1^N (\text{Model} - \text{Obs})}{\sum_1^N (\text{Obs})} \times 100\%$
Root mean square error (RMSE)	$RMSE = \sqrt{\frac{1}{N} \sum_1^N (\text{Model} - \text{Obs})^2}$
Unpaired peak accuracy (UPA)	$UPA = \frac{\text{Model}_{\max} - \text{Obs}_{\max}}{\text{Obs}_{\max}} \times 100\%$
Accuracy (<i>A</i>)	$A = \left(\frac{b+c}{a+b+c+d} \right) \times 100\%$
Critical success index (CSI)	$CSI = \left(\frac{b}{a+b+d} \right) \times 100\%$
Probability of detection (POD)	$POD = \left(\frac{b}{b+d} \right) \times 100\%$
Bias (<i>B</i>)	$B = \left(\frac{a+b}{b+d} \right)$
False alarm ratio (FAR)	$FAR = \left(\frac{a}{a+b} \right) \times 100\%$

^aModel: modeled (data obtained from simulations); Obs: observations (ambient data); *N*: number of observations; *a*: forecast of an exceedance that did not occur; *b*: forecast of an exceedance that occurred; *c*: forecast of a non-exceedance that did not occur; *d*: non-forecast of an exceedance that occurred.

are associated with local-regional episodes of air pollution in the NEIP that result in high levels of O₃ (Barros et al., 2003) and particulate matter during summer. Maximum O₃ levels in Catalonia are estimated in Plana de Vic (VIC) and the Alcover (ALC) industrial zone (over 94 ppb, 189 μg m⁻³) (Fig. 2). At night, the offshore flows produced drainage of pollutants towards the coast through the river valleys. As the day advanced, a well developed sea-breeze regime established along all the domain with breeze circulation cells up to 2000 m height, over the mixing height (800 m) (Sicard et al., 2003). At the leading edge of the sea breeze front, breezes converge with upslope winds to inject a fraction of these pollutants in their return flows aloft. Once in those upper layers, pollutants move back toward the sea (Baldasano et al., 1994) and the air at the middle troposphere is forced to go down by the subsidence over the east coast (Millán et al., 1992). In the low levels, the air masses recirculate over the sea with a possible later return to the seaboard. At noon, pollutants departing from the Barcelona area, as the main emitter zone, and the coastline are transported inland following the breeze front and the main orographic canalizations. Around 2000 UTC, the photochemical activity ceases, the sea-breeze regime loses intensity and winds in the coast weaken.

4. Results of MM5-EMICAT2000-CMAQ evaluation

4.1. Evaluation of the performance of meteorological fields for 13–16 August 2000

Grid size is influenced primarily by local topography (Salvador et al., 1999). Topographical variations can have an important effect on mesoscale atmospheric flow and, therefore, although topography is not the only driving mechanism that contributes to the dispersion of pollutants in the given domain, it plays a major role and should be well resolved in modeling exercises. Fig. 3 represents the topographic map of the domain and MM5-simulated wind fields at an 8, 4 and 2 km grid spacing for 14 August 2000. There are several significant differences between the coarse and fine topography. Nevertheless, it should be considered that smoothing is sometimes necessary to avoid the strong topographical gradients that may not be properly resolved by the models (McQueen et al., 1995).

Results depict that important mesoscale phenomena within the region do not develop in the study domain if the horizontal resolution is coarser than 4 km (Fig. 3). The sea breeze development is well captured by all simulations, even though; particular canalizations of the flow are only appreciable at 4 and 2 km grid spacing. Coarse resolution does not manage to describe the complexity observed in the emission pattern (Fig. 4). In the Pyrenees, the influence of resolution is more stressed with incrementing resolution to 2 km. The vertical structure of the flows is also influenced by the best representation of the topography when working with high horizontal resolution. An enhancement of vertical motions is observed, and the vertical structure of the sea breeze is improved, and several orographic injections appear when increasing the resolution. Down-slope and down-valley winds in the Pyrenees valleys at night are observable in the finest grid but are not described by the 8 or 4 km grid (Fig. 5).

Table 2 shows the root mean square error (RMSE) of wind speed at 10 m, for the lower, middle and upper troposphere and RMSE of wind direction at 10 m, in the case of different horizontal grid spacing. The general behavior of the model shows a tendency to overestimate nocturnal surface winds and to underestimate the diurnal flow. A clear improvement is produced in the direction of the winds with 2 km simulation during the central part of the day. The complex structure of the sea breeze described by the 2 km simulation, and the development of up-slope winds appears to agree in a higher grade with surface measurements. The statistics show how the model presents a better behavior within the PBL, and major disagreement with the radiosonde appears over 1000 m above ground level. At night, 8 and 4 km presents better results aloft, while at noon the high horizontal resolution simulation obtains the best statistics.

A more detailed analysis has been done for 14 August 2000 for the finest resolution (2 km). If the radiosonde is used to evaluate aloft results (Table 3), maximum MAGE for wind speeds is 3.22 m s⁻¹ in the high troposphere. In the middle and upper troposphere, the temperature is overestimated. In these layers, errors are under those of the PBL, because of the accuracy in the description of synoptic processes aloft, that is higher than the development of mesoscale phenomena within the PBL. Table 3 also presents a more detailed analysis of the mean bias of the wind speed and the RMSE

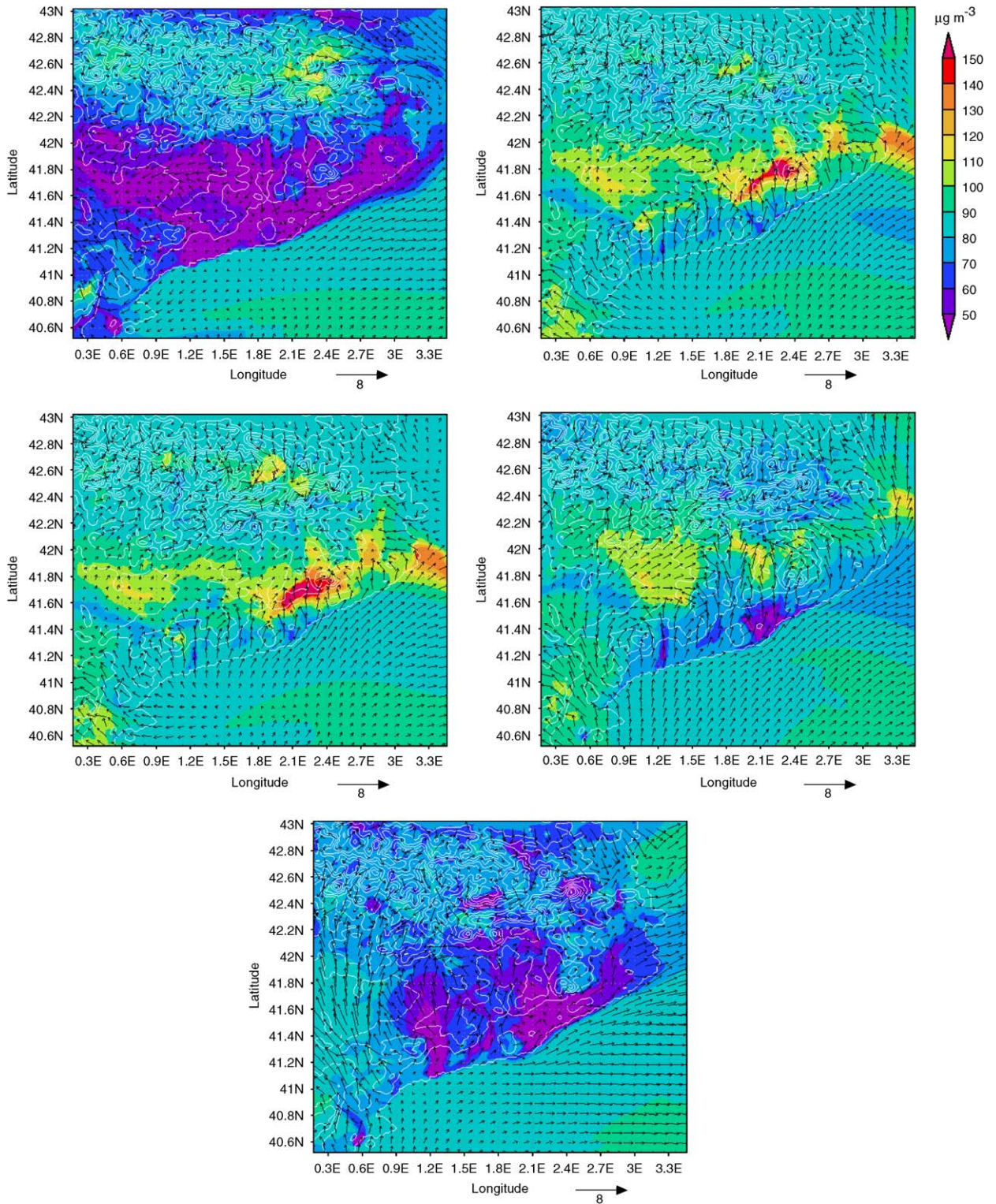


Fig. 2. Ozone concentrations ($\mu\text{g m}^{-3}$) and wind field vectors at ground-level over the northeastern Iberian Peninsula simulated with MM5-EMICAT2000-CMAQ on 14 August 2000, at (from left–right and top–bottom) 0600, 1100, 1200, 1600 and 2000 UTC.

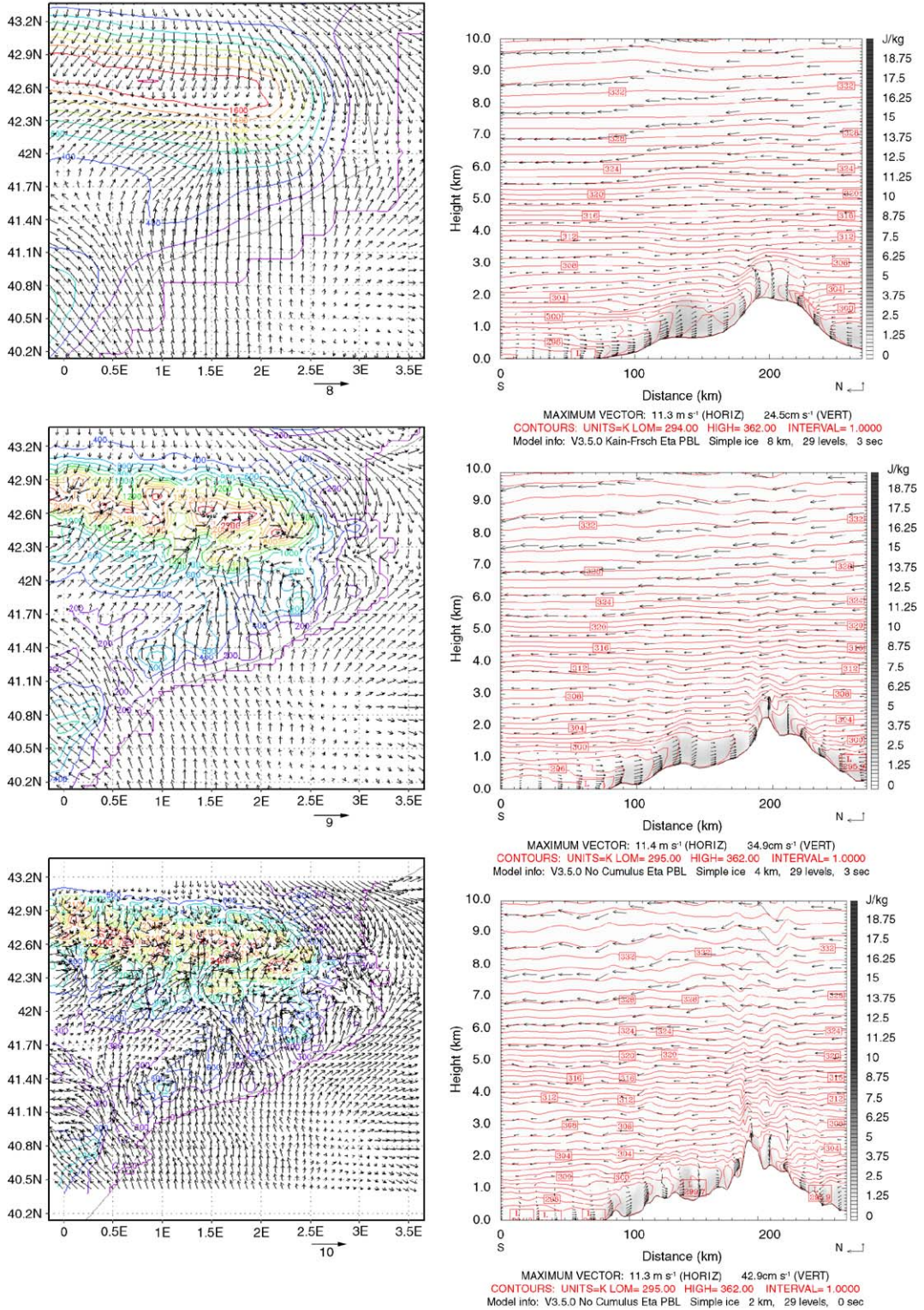


Fig. 3. Surface wind field in the northeastern Iberian Peninsula (left) and vertical profile Mediterranean Sea–Barcelona–the Pyrenees (right) for 14 August 2000, at 1200 UTC: 8-km grid (top), 4-km (center) and 8-km grid (bottom).

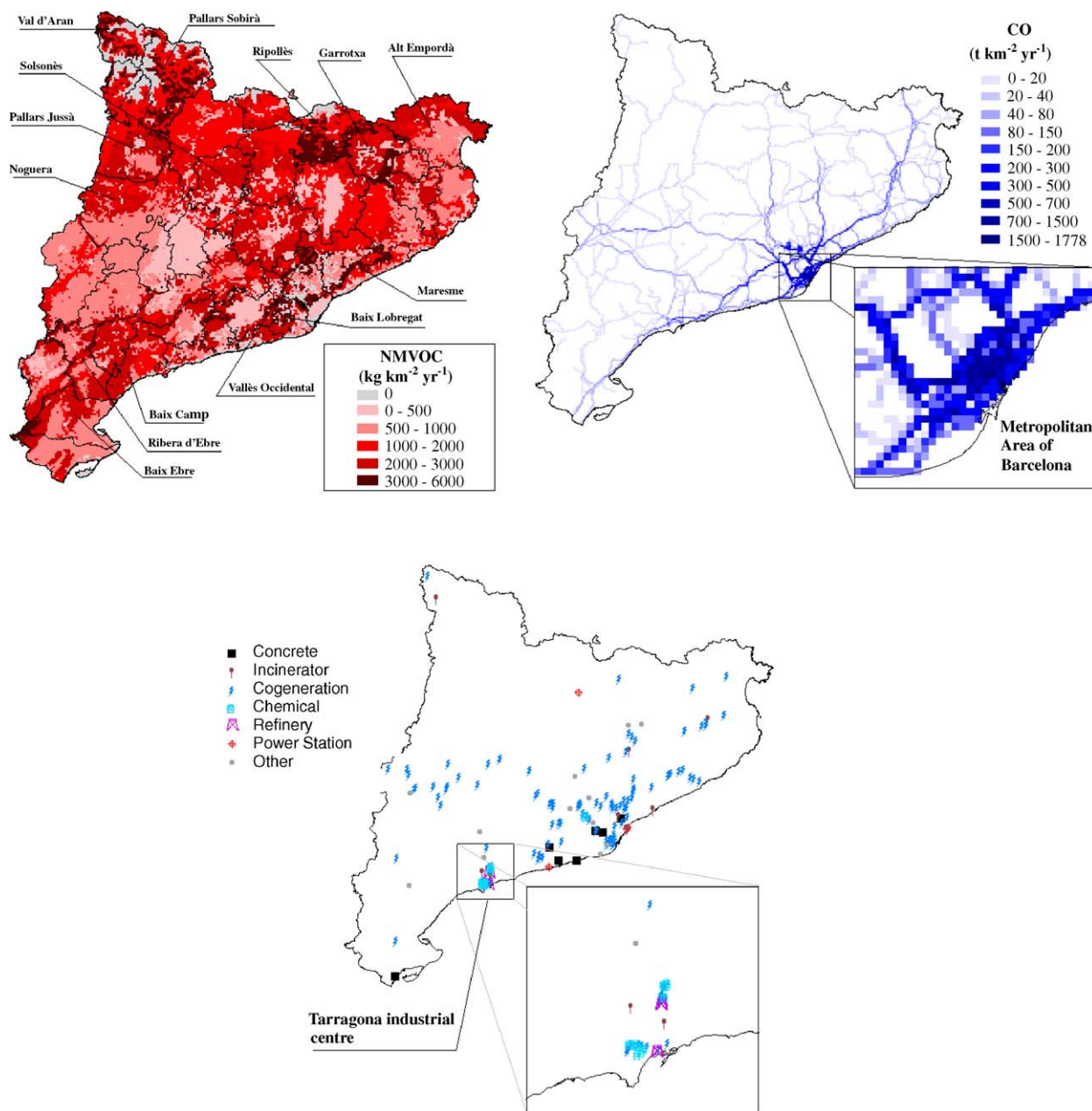


Fig. 4. Emissions included in EMICAT2000: (upper-left) biogenic NMVOCs emissions in the northeastern Iberian Peninsula during 2000. Main emitter sources are shrub lands, coniferous and deciduous forest; (upper-right) CO emission distribution due to on-road traffic during the year 2000; and (bottom) location and type of industrial sources.

in the wind direction for the grid spacing of 2 km. During daytime, biases in wind speeds are kept around 3 m s^{-1} . Inland areas present a good fit with observations, with a slight tendency to underpredict wind speeds. Simulated winds are excessively intense in some coastal locations and the Pyrenees. Wind direction presents highest deviations during night-

time due to the problems to accurately simulate low intensity winds. At noon, flows are underestimated and, on the other side, the behavior of direction is well captured by simulations.

With respect to temperature, the MAGE only exceeds the 3.3°C at 1200UTC in the PBL. Main differences are met in the lower troposphere, with a

Table 2

RMSE statistic of wind speed, and wind direction for 2-, 4-, 8-km simulations at 00, 12, 24 UTC during the episode of 13–6 August, 2000 (surface values evaluated with 52 surface stations, aloft values evaluated with a radiosonde)

	00 UTC			12 UTC			24 UTC		
	2 km	4 km	8 km	2 km	4 km	8 km	2 km	4 km	8 km
<i>RMSE wind speed ($m s^{-1}$)</i>									
Surface 10 m	1.71	1.85	1.76	2.04	2.34	2.41	2.00	2.17	2.22
Radiosonde < 1000 m	0.84	1.02	1.04	1.04	1.08	1.34	1.31	0.86	0.86
1000–5000 m	5.03	3.95	3.66	1.55	2.4	2.16	3.7	2.59	2.27
5000–10000 m	8.45	8.92	8.62	5.15	6.22	6.3	3.94	5.29	5.16
<i>RMSE wind direction (deg)</i>									
Surface 10 m	95.95	91.33	92.10	44.74	58.17	55.25	89.40	98.59	94.69

Table 3

Statistical summary of the behavior of temperature, wind speed and wind direction for meteorological simulations with a horizontal grid spacing of 2 km evaluated with a radiosonde in the city of Barcelona for 14 August, 2000

Height (m)	RMSE			MAGE			MNGE			MB		
	00 UTC	12 UTC	24 UTC	00 UTC	12 UTC	24 UTC	00 UTC	12 UTC	24 UTC	00 UTC	12 UTC	24 UTC
<i>Temperature ($^{\circ}C$)</i>												
5000/10000	2.63	2.15	2.10	2.58	2.04	1.76	0.14	0.14	0.12	2.58	2.04	1.73
1200/5000	1.85	1.53	1.39	1.83	1.29	1.18	0.55	0.46	0.25	1.83	1.29	1.11
<1200	2.45	3.69	3.22	2.21	3.39	2.98	0.09	0.13	0.12	-2.11	-3.39	-2.98
<i>Wind Speed ($m s^{-1}$)</i>												
5000/10000	4.12	2.49	3.81	3.22	2.14	3.16	1.01	1.13	1.20	-1.74	-1.78	-3.16
1200/5000	2.78	2.13	2.30	2.17	1.78	2.00	0.60	1.32	0.86	1.95	-1.77	1.20
<1200	2.71	3.26	1.12	2.39	3.14	0.94	1.40	1.60	1.12	-2.13	-3.14	-0.50
<i>Wind Direction (deg)</i>												
5000/10000	7.24	12.16	16.08	6.58	9.35	14.54	0.92	0.75	0.66	-1.07	-8.41	-12.24
1200/5000	53.85	73.24	22.89	29.71	54.29	15.34	—	0.78	1.05	-28.90	-54.26	-3.62
<1200	94.10	62.78	75.94	78.50	56.39	62.03	0.85	0.62	1.25	-7.00	-56.39	10.20

clear tendency to underestimate the temperature in these layers, as indicated by mean bias and MAGE, which present equal values.

4.2. Evaluation of CMAQ chemical transport model

4.2.1. Evaluation of the influence of grid resolution in CMAQ

Ground-level O_3 simulation results for different horizontal and vertical resolutions were compared to the measurements from 48 surface stations in the NEIP, located in both urban and rural areas, for 1-h peaks of O_3 . Table 4 collects the results of the statistical analysis using US EPA (1991) recommendations for the whole episode of 13–16 August 2000; Suggested values of ± 10 –15% for MNBE,

± 15 –20% for the UPA and +30–35% for the MNGE to be met by modeling simulations of O_3 have been considered for regulatory applications (Russell and Dennis, 2000; Hogrefe et al., 2001).

Progressively decreasing the grid spacing from 8 to 2 km (Fig. 5) improves the performance of all statistical parameters. The MNBE is negative for every simulation, ranging from -16.92% for 4 km/16 layers to -2.02% for 2 km/6 layers case. The MNGE is similar in all cases studied, being within the aforementioned standards. The UPA does not greatly improve when decreasing the grid spacing from 8 to 4 km, but this improvement becomes evident in the 2 km/16 layers simulation. The measured episode peak (94.5 ppb) is well-captured by the model with a 2 km/16 layers resolution,

Table 4

Summary results for evaluation of O₃ concentrations with different horizontal and vertical resolutions for the episode of 13–16 August 2000

Observed peak (ppb)	94.5					
Modeled peak (ppb)	103.4	94.0	65.6	71.5	68.3	72.0
	2 km/6 layers	2 km/16 layers	4 km/6 layers	4 km/16 layers	8 km/6 layers	8 km/16 layers
<i>Discrete evaluation</i>						
UPA (%)	9.64	−0.76	−30.76	−24.37	−27.45	−23.67
MNBE (%)	−2.02	−11.38	−9.53	−16.92	−12.86	−13.12
MNGE (%)	19.72	20.89	17.42	21.61	19.27	21.01
<i>Categorical evaluation</i>						
A (%)	90.9	91.6	91.5	92.4	91.6	91.7
B (%)	0.7	0.3	0.1	0.1	0.1	0.3
CSI (%)	19.0	12.5	3.2	8.9	3.2	10.0
POD (%)	26.4	14.9	3.4	9.2	3.4	11.5
FAR (%)	59.6	56.7	72.7	27.3	70.0	56.5

yielding values of −0.76% for the unpaired peak accuracy. The effects of grid resolution on the chemistry of O₃ and NO_x are far more important than the chemistry of VOCs (Jang et al., 1995). The predicted first layer O₃ and NO_x concentrations by 6- and 16-layer vertical resolutions are distinctively different for the whole domain. Ozone predictions from the 6-layer case show slightly higher values than those from the 16-layer model; meanwhile NO_x concentrations (Table 5) are significantly higher in the case of 16-layer vertical resolution. This can be explained by the fact that the VOCs and NO_x emissions injected into the 6-layer model are diluted in a deeper layer compared to the same injected into the 16-layer model. Since most of the domain presents a VOCs-limited sensitivity (Jiménez and Baldasano, 2004), increasing NO_x concentration in the first layer presents the contrary effect on tropospheric O₃, producing less O₃ from the photochemical reaction and lowering ground-level O₃ concentrations. This might also be occurring due to higher titration of O₃ as a consequence of a higher NO concentration. As shown in Table 5, coarser cell sizes are too large to correctly represent NO_x emissions, which have very distinctive grid-scale distributions; the result of photochemical reactions with diluted primary species concentrations does not give a similar range as observed O₃ concentrations. In addition, performance of the model greatly improves when using 16 vertical layers instead of just six layers. The 8 km resolution tempers the concentrations of pollutants, yielding

most of values in a medium range, not capturing the extreme values (maximum and minimum levels of NO_x) that are more truthfully predicted by the finer resolution. The limited range in the daily O₃ concentrations is related to the over-smoothing of NO_x emission rates in the model with coarse horizontal and vertical resolutions. Nitrogen oxides species is more sensitive than O₃ to model grid structure since secondary species have more horizontal homogeneity than primary species.

With respect to categorical forecasting for O₃, statistical parameters indicate that the *A* (percent of forecasts that correctly predict an exceedance or non-exceedance) is above 90% for every resolution, but yielding the best parameters for the 16-vertical layers resolution compared to the higher vertical grid spacing. Since this metric can be greatly influenced by the overwhelming number of non-exceedances, to circumvent this inflation the CSI and the POD is used. Both parameters perform similarly during the episode, yielding more accurate values when using a 2 km resolution. The value of *B* (*B* < 1 for all simulations) indicates that exceedances are generally underpredicted for every resolution, which corresponds with the value of MNBE obtained for discrete evaluations, but this underprediction is minor for the 2 km/6 layers case (0.7) and the 2 km/16 layers case (0.3). Last, the fifth categorical parameter, the FAR, indicated the number of times that the model predicted an exceedance that did not occur. This metric is higher

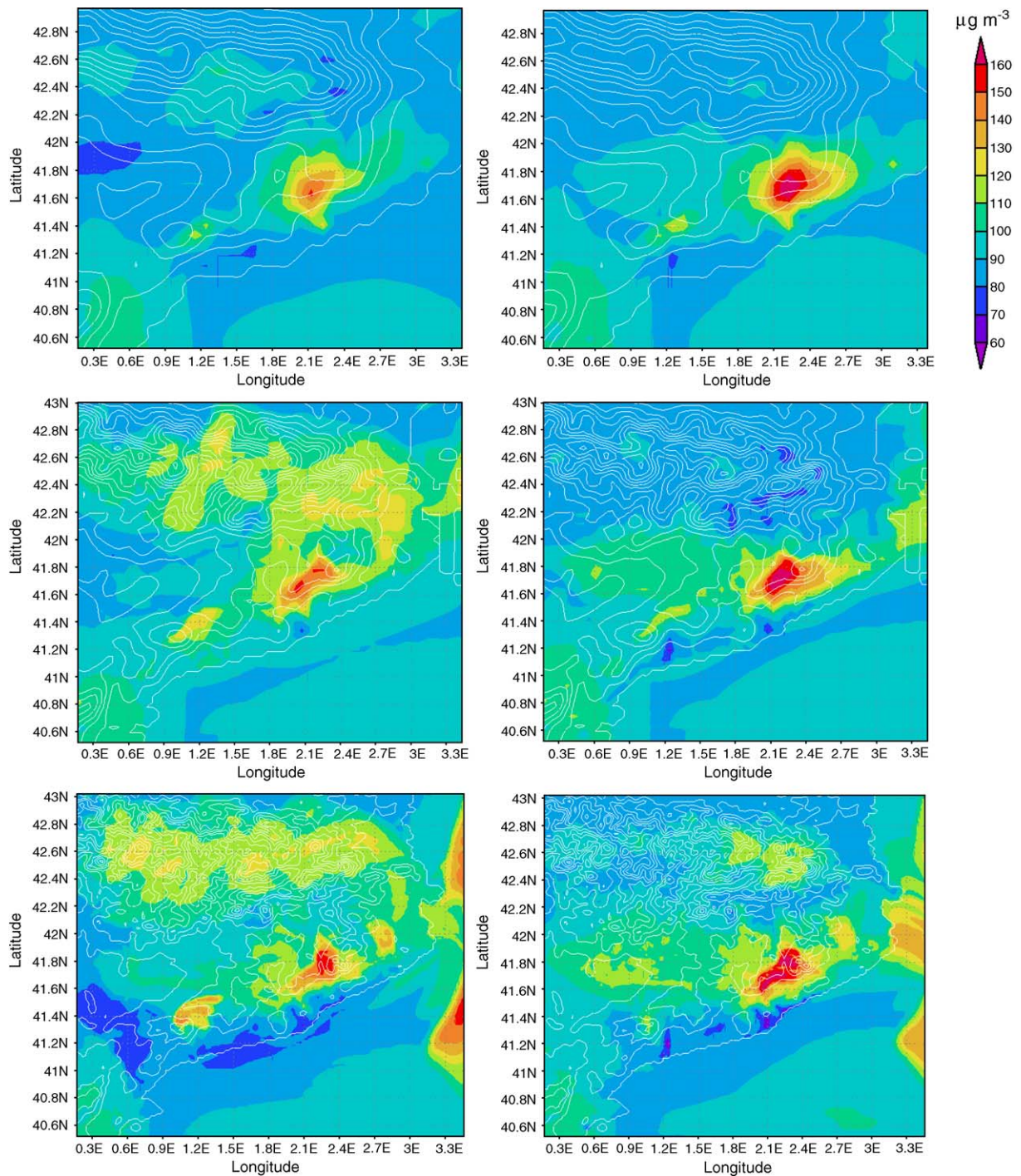


Fig. 5. One-hour maximum O₃ levels ($\mu\text{g m}^{-3}$) in the simulation domain for an 8-km (top), 4-km (center) and 2-km (bottom) horizontal resolution with 6 (left) and 16 (right) vertical layers for the episode of 13–16 August 2000.

for the simulations with inferior vertical resolution (above 70% for the 4 km/6 layers and the 8 km/6 layers cases), because of the possible influence of the vertical collapse of emissions, which can be high for

the sum of precursor species for O₃. Thus, a grid spacing of 2 km/16 layers was selected for performing subsequent simulations of air quality issues in the NEIP.

Table 5
Summary results for evaluation of NO_x concentrations with different horizontal and vertical resolutions

Observed peak (ppb)	110.0					
Modeled peak (ppb)	74.5	123.5	76.9	95.1	40.2	70.5
	2 km/6 layers	2 km/16 layers	4 km/6 layers	4 km/16 layers	8 km/6 layers	8 km/16 layers
MNBE (%)	−28.64	9.46	−23.34	−17.77	−52.32	−32.78
MNGE (%)	39.20	31.36	40.76	41.75	39.73	37.78
UPA (%)	−32.20	12.36	−30.13	−13.54	−63.86	−36.10

Table 6
Statistical measures of model performance for 1-h O₃ during the episode of August 13–16 2000 for a grid spacing of 2 km/16 vertical layers

	EPA Goal	August 13 2000	August 14 2000	August 15 2000	August 16 2000
<i>Discrete evaluation</i>					
Observed peak (ppb)		78.5	88.5	94.5	85.5
Modeled peak (ppb)		94.0	84.9	83.5	90.1
UPA (%)	< ±20%	14.4	−3.8	−11.7	5.2
MNBE (%)	< ±15%	−2.1	−11.0	−14.3	−5.6
MNGE (%)	<35%	16.8	19.8	21.7	26.7
<i>Categorical evaluation</i>					
A (%)		91.1	92.2	90.0	89.7
B (%)		0.7	0.1	0.1	0.4
POD (%)		22.1	6.9	9.6	11.5
CSI (%)		15.0	6.7	9.2	9.1
FAR (%)		67.9	33.3	31.3	69.6

4.2.2. Day-to-day evaluation of ozone during the 13–16 August 2000 episode

Table 6 shows the results of both the discrete and categorical statistical analysis detailed for each day of the episode of photochemical pollution of 13–16 August 2000 with the highest resolution considered in this work (2 km for horizontal grid and 16 vertical layers). The model results achieve the US EPA (1991) goals for a discrete evaluation on all episode days. The O₃ MNBE is negative on each day, ranging from −2.1% on the first day of simulation to −14.3% on August 15. That suggests a slight tendency towards underprediction; however, USEPA goals of ±15% are achieved. This negative bias may suggest that the O₃-production chemistry may not be sufficiently reactive. The UPA is overestimated on the first and last days of the simulations (14.4% and 5.2%, respectively) and underestimated on the central days of the episode (−3.8% and −11.7%). The MNGE increases from August 13 until August 16 (16.8–26.7%), mainly

due to deviations in meteorological predictions that enlarge with the time of simulation (Jiménez et al., 2005a). The objective set in the Directive 2002/3/EC (deviation of 50% for the 1 h averages) is also achieved for the whole period of study. With respect to categorical forecasting, statistical parameters indicate that the *A* (percent of forecasts that correctly predict an exceedance or non-exceedance) is around 90% for every day of simulation, decreasing the performance by the end of the episode. The CSI and the POD yield more accurate values when O₃ peaks are higher (and when exceedances of the 60 ppb threshold taken as reference are more frequent). The value of *B* (*B*<1 for all simulations) indicates that exceedances are generally underpredicted, which corresponds with the value of MNBE obtained for discrete evaluations. Last, the FAR is high for the first and last day of the simulations (around 68%), because of the possible initialization influence during the first moments of simulation, that can be high for the sum of reservoir species for

O₃ (Berge et al., 2001); and the errors attributable to the meteorology, that accumulate over the period and perturb through the forecasts.

4.2.3. Other statistical parameters for ozone and its precursors (NO_x and CO)

Table 7 indicates the results of the evaluation of MM5-EMICAT2000-CMAQ with different statistical parameters for O₃, CO and NO_x against ambient data. Evaluation against 1649 measurements is performed in the case of O₃; results show a correlation of 0.74 between simulations and ambient data. The mean bias (0.5 ppb for CMAQ) indicates a tendency to overprediction of values. The RMSE is also low for the regional simulations (6.7 ppb). Simulations for CO and NO_x tend to

show much larger bias and error than the similar statistics of O₃ for the same simulation. As noted by Russell and Dennis (2000), currently air quality models show a pervasive tendency towards underprediction of precursors. Despite there are no references in the goals to be achieved in the evaluation of O₃ precursors predicted by air quality models, results with bias between –20% and –50% are accepted (Russell and Dennis, 2000). In the case of NO_x, results of –9.2% for the normalized mean bias are met, while the MNBE is 6.1%. The correlation coefficient between the observed and predicted NO_x concentrations at 48 stations is 0.75 for CMAQ. The RMSE is 20.2 ppb for the regional model for NO_x predictions in the domain of the NEIP. In the case of CO, the correlation coefficient

Table 7

Statistical evaluation of photochemical pollutants (O₃, NO_x and CO) in the northeastern Iberian Peninsula during the episode of 13–16 August, 2000

	Observations	Simulated		
<i>Ozone</i>				
Mean (ppb)	31.8	32.4	<i>N</i>	1649
SD (ppb)	18.7	15.7	Coefficient of correlation (<i>R</i>)	0.74
CV (%)	58.7	48.6	MB (ppb)	0.52
Max. (ppb)	94.5	94.0	MNBE (%)	37.9
95th (ppb)	61.5	57.0	MFB (%)	5.6
75th (ppb)	46.0	41.8	MAGE (ppb)	4.9
50th (ppb)	30.5	33.4	MNGE (%)	64.1
25th (ppb)	16.5	21.5	NME (%)	30.8
5th (ppb)	4.6	5.0	NMB (%)	1.7
Min. (ppb)	0.5	0.0	RMSE (ppb)	6.7
<i>Nitrogen oxides</i>				
Mean (ppb)	34.0	30.9	<i>N</i>	907
SD (ppb)	26.0	29.5	Coefficient of correlation (<i>R</i>)	0.75
CV (%)	76.4	95.6	MB (ppb)	–3.11
Max. (ppb)	159.6	161.7	MNBE (%)	6.1
95th (ppb)	85.2	94.1	MFB (%)	–23.8
75th (ppb)	45.4	41.9	MAGE (ppb)	15.0
50th (ppb)	27.2	21.4	MNGE (%)	62.7
25th (ppb)	15.8	9.6	NME (%)	44.4
5th (ppb)	5.6	2.1	NMB (%)	–9.2
Min. (ppb)	1.6	0.7	RMSE (ppb)	20.2
<i>Carbon monoxide</i>				
Mean (ppb)	476.8	437.7	<i>N</i>	907
SD (ppb)	396.8	340.3	Coefficient of correlation (<i>R</i>)	0.74
CV (%)	83.2	77.8	MB (ppb)	–26.88
Max. (ppb)	2300.0	2306.9	MNBE (%)	7.0
95th (ppb)	1400.0	1198.2	MFB (%)	–2.7
75th (ppb)	550.0	519.8	MAGE (ppb)	125.7
50th (ppb)	350.0	321.0	MNGE (%)	30.3
25th (ppb)	200.0	219.7	NME (%)	38.4
5th (ppb)	200.0	184.6	NMB (%)	–8.2
Min. (ppb)	100.0	138.0	RMSE (ppb)	208.1

between the observed and predicted carbon monoxide concentrations for the 907 observation values during this episode is 0.74, and hence correlating worse than O₃ and NO_x in the study domain. The mean bias is −26.9 ppb (MNBE of 7.0%) and the RMSE is 208.1 ppb for CMAQ. Summarizing, the simulation with the CMAQ underestimates maximum O₃, CO and NO_x levels with regards to ambient data, since the grid resolution highly influences the formation and loss processes of pollutants (especially photochemistry and vertical transport). Hence, the average volume defined by the model's horizontal grid spacing must be sufficiently small to allow the air quality to be reproduced accurately (Jiménez et al., 2005a).

4.3. Evaluation of the sensitivity of MM5-EMICAT2000-CMAQ to emission reductions

Sensitivity studies provide the opportunity to check whether O₃ values react consistently to similar changes in emissions. The effect of reducing O₃ precursors on sensitivity regimes was evaluated performing simulations for the domain with baseline emission rates for VOCs and NO_x as derived from EMICAT2000 model, and reducing anthropogenic VOCs and NO_x emissions by 35% following the methods of Milford et al. (1994), Sillman (1995) and Sillman et al. (2003). Meteorology represents the same day in order not to introduce any external influence. Three inner scenarios of 32 × 32 km² were deeply analyzed on 14 August 2000, at 1200 UTC, the hour of maximum ground-level O₃ production: (a) an urban area that comprises the Barcelona Geographical Area (BGA); (b) a background area centered in VIC; and (c) an industrial zone centered in ALC. The selection of these scenarios came conditioned because these areas present important photochemical pollution episodes in the NEIP. Results indicate (Fig. 6) that areas downwind the city of Barcelona benefit from NO_x reductions (reduction of 10 ppb in ground-level O₃), meanwhile the same reduction causes an important increment of O₃ in Barcelona (9 ppb) and the area downwind Tarragona (18 ppb), with a high industrial influence. The city of Barcelona benefits from VOC reductions (10 ppb of O₃), as well as the industrial zone of ALC (20 ppb). The rest of the domain is practically insensitive to VOC reductions. Ozone chemistry in the plume arriving at VIC is close to the transition between VOC-sensitive and NO_x-sensitive condi-

tions. Nevertheless, BGA and ALC present highly VOC-sensitive behavior due to the significant traffic and industrial NO_x emissions. Predicted NO_x-VOC sensitivity varies considerably among the three model scenarios; the varying NO_x-VOC predictions occur despite O₃ being similar in all three scenarios. Table 8 shows the results of the evaluation of ground-level O₃. Peak O₃ in the different scenarios is slightly lower than the measured values for each considered case. Comparison between model and measurements shows a good agreement when the model predicts dominant VOC-sensitive chemistry in the BGA and ALC scenarios. Here, statistical parameters of O₃ evaluation worsen when reducing VOCs emissions and improve in the −35% NO_x case, especially in the BGA, where UPA reduces from −18% in the VOC-reduction case to −8% in the NO_x-reduction case. The same behavior is observed in ALC. By contrast, the evaluation in VIC depicts a clear underprediction of O₃ levels (around −18% of MNBE, 27% of MNGE and −13% of UPA). Statistic parameters in the stations of VIC worsen when reducing precursor emissions by 35%, especially in the case of 35% NO_x reduction, that yields to a more important underestimation of O₃ levels in the area because of the NO_x-limited regime of this scenario. Model-measurement comparison suggests that the O₃-production chemistry may not be sufficiently reactive, possibly because of an underestimation in reactive VOC and/or an overestimation in NO_x emissions.

5. Conclusions

The application of air quality models in complex terrain leads to the necessity of using high-resolution applications that must be conveniently evaluated. Results presented in this work contribute to the assessment of MM5-EMICAT2000-CMAQ performance in urban, industrial and background scenarios over a complex terrain such as the NEIP. Application and exploitation of this air quality model in the area of study is conditioned to the potential adaptation of meteorological and emission tools; nevertheless, flexibility of the model allows the use of specific models developed with additional tools and according to the proper characteristics of the zone, which can be used as a more accurate alternative.

Outputs from the chemical transport model were sensitive to the grid size employed in the simulations, presenting a higher dependence on horizontal grid than on the vertical resolution when simulating

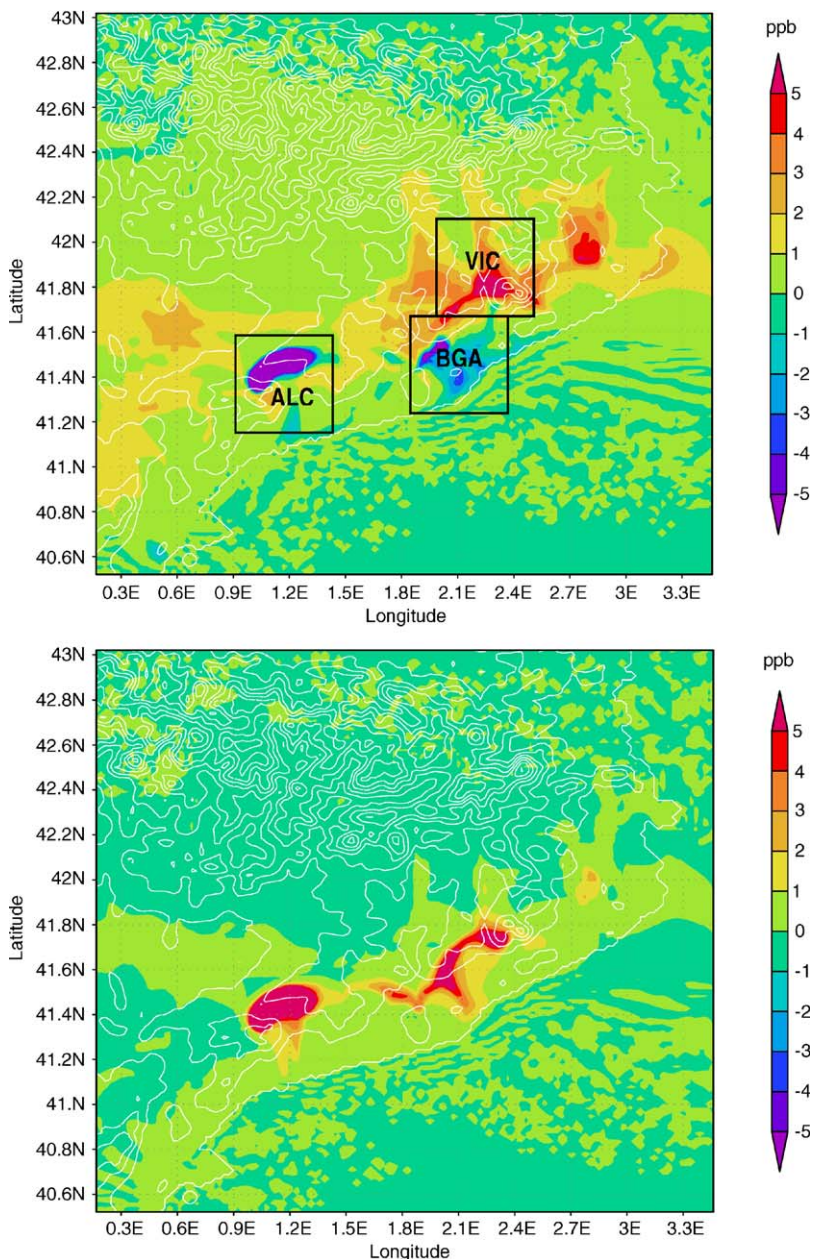


Fig. 6. Reduction in peak O_3 concentrations (ppb) at 1200 UTC of 14 August 2000, due to; (top) 35% reduction in NO_x emissions (base case— NO_x reduction case); and (bottom) 35% reduction in VOCs emissions (base case—VOCs reduction case). Positive values imply O_3 reductions with respect to the base case. Differences over 2 ppb indicate NO_x - or VOC-sensitive regimes.

O_3 ; nevertheless, high vertical resolution was found to be as important as horizontal resolution to properly simulate other photochemical pollutants such as NO_x . Despite in outline the dynamics of photochemical pollutants as O_3 and the patterns of its precursors do not change dramatically, some small-scale features appear when using a grid spacing of 2 km that cannot be captured with

coarser horizontal resolutions. The large averaging volumes used by regional models are feared to lead to unacceptable errors for many species that are formed via nonlinear chemical reactions (e.g. O_3 and its precursors), particularly in areas with significant chemical gradients. Meanwhile having a finer grid is important for addressing O_3 processes in urban and industrial areas, rural areas allow

Table 8

Evaluation of the sensitivity of O₃ concentrations to emission reductions in scenarios of the domain presenting different O₃–NO_x–VOC sensitivity: Barcelona (urban), Vic (background) and Alcover (industrial)

Max. measured (ppb)	49.0		
	Base case	–35% NO _x	–35% VOC
<i>Barcelona geographical area (Urban)</i>			
Max. simulated (ppb)	42	45	40
MNBE (%)	–17.31	–10.16	–19.36
MNGE (%)	24.11	23.76	28.16
UPA (%)	–13.56	–7.94	–17.52
Max. measured (ppb)	88.0		
<i>Plana de Vic (background)</i>			
Max. simulated (ppb)	77	71	75
MNBE (%)	–18.64	–19.69	–22.02
MNGE (%)	27.62	31.16	28.39
UPA (%)	–12.90	–19.84	–15.14
Max. measured (ppb)	64.0		
<i>Alcover (Industrial)</i>			
Max. simulated (ppb)	58	60	56
MNBE (%)	–14.07	–11.75	–15.68
MNGE (%)	19.58	19.31	20.20
UPA (%)	–8.31	–5.12	–11.47

larger grids to capture the non-linearity of the chemical processes. However, successful results are currently being obtained when modeling some important O₃ pollution episodes in the NEIP, which demand high spatial resolution both from emissions and meteorology.

The simulations with a resolution of 2-km and 16 vertical layers show a good behavior with respect to the statistical figures analyzed. The objective set in the Directive 2002/3/EC is achieved for the whole period of study for MM5-EMICAT2000-CMAQ simulations. The model meets the objective of ±20% set by USEPA for prediction of the peak levels of O₃ during the episode. Thus, simulation of the NEIP with 2 km/16 layers resolution is a reliable methodology that provides the possibility of describing the dynamics and processes of pollutants on a regional scale.

In addition, results provided a preliminary approach to the assessment of O₃–NO_x–VOC sensitivity in the NEIP during a typical re-circulation episode of photochemical pollution. The O₃ chemistry in the Barcelona city plume arriving at VIC (downwind area) is close to NO_x-sensitive conditions. Nevertheless, the urban area of Barcelona and

the industrial zone of ALC present highly VOC-sensitive behavior due to the significant traffic and industrial NO_x emissions. When comparing simulation results with ambient data, the underestimation of VOC and/or an overestimation in NO_x emissions may cause the O₃-production chemistry not to be sufficiently reactive. The model evaluation shown here is relatively simple to perform and provides a test for sensitivity evaluation and is the first step for establishing control policies for ozone-precursor emissions; however, it is highly conditioned to the lack of availability of ambient data in the NEIP.

Acknowledgements

This work was developed under the research contract REN2003-09753-C02 of the Spanish Ministry of Science. The Spanish Ministry of Education is also thanked for the FPU doctoral fellowship held by P. Jiménez. The authors gratefully acknowledge E. López for the implementation of EMICAT2000 into a GIS system. Air quality stations data and information for implementing industrial emissions were provided by the Environmental Department of the Catalonia Government, Spain.

References

- Baldasano, J.M., Cremades, L., Soriano, C., 1994. Circulation of air pollutants over the Barcelona Geographical Area in summer. In: Proceedings of the Sixth European Symposium on Physico-Chemical Behaviour of Atmospheric Pollutants, Varese, Italy, 18–22 October, 1993. Report EUR 15609/1, pp. 474–479.
- Barros, N., Toll, I., Soriano, C., Jiménez, P., Borrego, C., Baldasano, J.M., 2003. Urban photochemical pollution in the Iberian Peninsula: the Lisbon and Barcelona airsheds. *Journal of the Air & Waste Management Association* 53, 347–359.
- Berge, E., Huang, H.-C., Chang, J., Liu, T.-H., 2001. A study of the importance of initial conditions for photochemical oxidant modeling. *Journal of Geophysical Research* 106, 1347–1363.
- Byun, D.W., Ching, J.K.S. (Eds.), 1999. Science algorithms of the EPA Models-3 Community Multiscale Air Quality (CMAQ) modeling system. EPA Report N. EPA-600/R-99/030, Office of Research and Development, US Environmental Protection Agency, Washington, DC.
- Dudhia, J., 1993. A nonhydrostatic version of the Penn State/NCAR mesoscale model: validation tests and simulation of an Atlantic cyclone and cold front. *Monthly Weather Review* 121, 1493–1513.
- Gery, M.W., Whitten, G.Z., Killus, J.P., Dodge, M.C., 1989. A photochemical kinetics mechanism for urban and regional scale computer modeling. *Journal of Geophysical Research* 94 (D10), 12925–12956.

- Hogrefe, C., Rao, S.T., Kasibhatla, P., Hao, W., Sistla, G., Mathur, R., McHenry, J., 2001. Evaluating the performance of regional-scale photochemical modeling systems: Part II—ozone predictions. *Atmospheric Environment* 35, 4175–4188.
- Jang, C.J., Jeffries, H.E., Byun, D., Pleim, J.E., 1995. Sensitivity of ozone to model grid resolution—I. Application of high-resolution regional acid deposition model. *Atmospheric Environment* 29 (21), 3085–3100.
- Jiménez, P., Baldasano, J.M., 2004. Ozone response to precursor controls: the use of photochemical indicators to assess O_3 – NO_x –VOC sensitivity in the northeastern Iberian Peninsula. *Journal of Geophysical Research* 109, D20309, doi:10.1029/2004JD004985.
- Jiménez, P., Jorba, O., Parra, R., Baldasano, J.M., 2005a. Influence of high-model grid resolution on photochemical modeling in very complex terrains. *International Journal of Environment and Pollution* 24(1/2/3/4), 180–200.
- Jiménez, P., Parra, R., Gassó, S., Baldasano, J.M., 2005b. Modeling the ozone weekend effect in very complex terrains: a case study in the northeastern Iberian Peninsula. *Atmospheric Environment* 39, 429–444.
- Jorba, O., Pérez, C., Rocadenbosch, F., Baldasano, J.M., 2004. Cluster analysis of 4-day back trajectories arriving in the Barcelona area (Spain) from 1997 to 2002. *Journal of Applied Meteorology* 43 (6), 887–901.
- Kang, D., Eder, B.K., Schere, K.L., 2003. The evaluation of regional-scale air quality models as part of NOAA's air quality forecasting pilot program. In: 26th NATO International Technical Meeting on Air Pollution Modeling and its Application, Istanbul, Turkey, pp. 404–411.
- Kang, D., Eder, B.K., Mathur, R., Yu, S., Schere, K.L., 2004. An operational evaluation of the ETA-CMAQ air quality forecast model. In: 27th NATO International Technical Meeting on Air Pollution Modeling and its Application, Banff, Canada, pp. 233–240.
- Kessler, Ch., Brücher, W., Memmesheimer, M., Kerschgens, M., Ebel, A., 2001. Simulation of air pollution with nested models in North Rhine-Westphalia. *Atmospheric Environment* 35 (Suppl. 1), S3–S12.
- McQueen, J.T., Draxler, R.R., Rolph, G.D., 1995. Influence of grid size and terrain resolution on wind field predictions from an operational mesoscale model. *Journal of Applied Meteorology* 34 (10), 2166–2181.
- Milford, J.B., Gao, D., Sillman, S., Blossey, P., Russell, A.G., 1994. Total reactive nitrogen (NO_y) as an indicator of the sensitivity of ozone to reductions in hydrocarbon and NO_x emissions. *Journal of Geophysical Research* 99 (D2), 3533–3542.
- Millán, M.M., Artiñano, B., Alonso, L., Castro, M., Fernandez-Patier, R., Goberna, J., 1992. Mesometeorological cycles of air pollution in the Iberian Peninsula. *Air Pollution Research Report 44*, Commission of the European Communities, Brussels, Belgium, p. 219.
- Ntziachristos, L., Samaras, Z., 2000. COPERTIII computer programme to calculate emissions from road transport. Methodology and emission factors (Version 2.1). Technical Report No. 49, European Environment Agency.
- Parra R., 2004. Development of the EMICAT2000 model for the estimation of air pollutants emissions from Catalonia and its use in photochemical dispersion modelling. Ph.D. Thesis, Technical University of Catalonia, <http://www.tdx.cesca.es/TDX-0803104-102139/> (in Spanish).
- Parra, R., Gassó, S., Baldasano, J.M., 2004. Estimating the biogenic emissions of non-methane volatile organic compounds from the North Western Mediterranean vegetation of Catalonia. *The Science of the Total Environment* 329, 241–259.
- Russell, A., Dennis, R., 2000. NARSTO critical review of photochemical models and modeling. *Atmospheric Environment* 34, 2283–2324.
- Salvador, R., Calbó, J., Millán, M.M., 1999. Horizontal grid size selection and its influence on mesoscale model simulations. *Journal of Applied Meteorology* 38, 1311–1329.
- Sicard, M., Pérez, C., Comerón, A., Baldasano, J.M., Rocadenbosch, F., 2003. Determination of the mixing layer height from regular lidar measurements in the Barcelona area. In: Schäfer, K.P., et al. (Eds.), *Remote Sensing of Clouds and the Atmosphere VIII*. Proceedings of the SPIE, vol. 5235, pp. 505–516.
- Sillman, S., 1995. The use of NO_y , H_2O_2 and HNO_3 as indicators for ozone– NO_x –hydrocarbon sensitivity in urban locations. *Journal of Geophysical Research* 100 (D7), 14175–14188.
- Sillman, S., Vautard, R., Menut, L., Kley, D., 2003. O_3 – NO_x –VOC sensitivity and NO_x –VOC indicators in Paris: results from models and atmospheric pollution over the Paris area (ESQUIF) measurements. *Journal of Geophysical Research* 108 (D17), 8563.
- Tesche, T.W., Lurmann, F.L., Roth, P.M., Georgopoulos, P., Seinfeld, J.H., Cass, G., 1990. Improvement of procedures for evaluating photochemical models. Report to California Air Resources Board for Contract No. A832-103, Alpine Geophysics, LLC, Crested Butte, CO.
- US EPA, 1991. Guideline for regulatory application of the urban airshed model. US EPA Report No. EPA-450/4-91-013, Office of Air and Radiation, Office of Air Quality Planning and Standards, Technical Support Division, Research Triangle Park, NC, US.